

Non-decoupling two-loop corrections to $(g - 2)_\mu$ from fermion/sfermion loops in the MSSM

H. G. Fagnoli^{a,b}, C. Gnendiger^a,
S. Paßehr^c, D. Stöckinger^a, H. Stöckinger-Kim^a

^a*Institut für Kern- und Teilchenphysik, TU Dresden, Dresden, Germany*

^b*Universidade Federal de Lavras, Lavras, Brazil and*

^c*Max-Planck Institut für Physik, München, Germany*

Two-loop contributions to the muon $(g - 2)$ from fermion/sfermion loops in the MSSM are presented, and an overview of the full MSSM prediction for $(g - 2)$ is given with emphasis on the behaviour in scenarios which are compatible with LHC data, including scenarios with large mass splittings. Compared to all previously known two-loop contributions, the fermion/sfermion-loop contributions can yield the largest numerical results. The new contributions contain the important universal quantities $\Delta\alpha$ and $\Delta\rho$, and for large sfermion masses the contributions are non-decoupling and logarithmically enhanced. We find up to 15% (30%) corrections for sfermion masses in the 20 TeV (1000 TeV) range.

I. INTRODUCTION

Supersymmetry (SUSY) is one of the best motivated ideas for physics beyond the Standard Model (SM) at the TeV scale. The anomalous magnetic moment of the muon $a_\mu = (g - 2)_\mu/2$ provides an important constraint on physics beyond the SM and a hint for low-energy SUSY. In the last decade, a discrepancy between the experimental value [1] and the SM prediction has continuously consolidated. It now amounts to

$$a_\mu^{\text{Exp-SM}} = (28.7 \pm 8.0) \times 10^{-10} \quad (1)$$

according to Ref. [2], based on the hadronic contributions of Ref. [3]. For further recent evaluations and reviews, see Refs. [4–6].

The deviation (1) can be explained very well by the extra contributions from low-energy SUSY in the minimal supersymmetric standard model (MSSM). However, a tension between a_μ , which prefers light SUSY particles, and LHC-results, which rule out certain MSSM parameter regions with light coloured SUSY par-

ticles, seems to develop. In the general MSSM there is no problem to accommodate all constraints simultaneously [7, 8], but in more specific models, such as the Constrained MSSM [9–11] or the scenarios of Refs. [12, 13] motivated by the little hierarchy problem, it has become impossible to explain the deviation (1). Hence the new experimental input has motivated the construction and analysis of many new SUSY models and scenarios. Some involve compressed spectra [14, 15] to allow lighter coloured SUSY particles without contradicting LHC limits. Some go beyond the MSSM and reconcile the Higgs mass with a_μ by lifting the Higgs mass with extra matter [16–18] or gauge bosons [19]. Many recently proposed models which stay within the MSSM framework involve rather split spectra, e.g. heavy coloured, light non-coloured SUSY particles [20–23], heavy third family, lighter first and second family [24], non-universal gaugino masses [25, 26], large Higgsino masses and large stop mixing from more generic gauge mediation

[27].

Not only the LHC data but also the a_μ measurement will improve soon. The Fermilab $g-2$ experiment [28, 29] is under construction. It aims to reduce the uncertainty by more than a factor four, down to 1.6×10^{-10} . At J-PARC [30] a complementary $g-2$ experiment with similar precision goal is planned. Clearly, pinning down the deviation (1) more precisely will lead to very valuable constraints on SUSY which are complementary to the ones from LHC data [6, 31].

The prospective experimental precision calls for similar improvements on the theory side, not only of the SM but also of the SUSY prediction for a_μ . The present theory error of the SUSY prediction has been estimated to 3×10^{-10} [32], almost twice as large as the future experimental uncertainty.

In this work we present results of a new calculation of an important class of SUSY two-loop contributions to a_μ : contributions where a fermion/sfermion loop is inserted into a SUSY one-loop diagram. Fig. 1 shows the generic diagram of this class, along with the SUSY one-loop diagrams. The computation of these diagrams is technically more demanding than the ones of the previously known two-loop contributions to a_μ . However, these two-loop fermion/sfermion-loop contributions are phenomenologically interesting particularly for split spectra because they are non-decoupling but logarithmically enhanced by heavy squarks. They further eliminate a significant source of theory uncertainty present in the one-loop contributions.

In the following we begin with an overview of the known contributions, stressing the variety of possibilities for large SUSY contributions to a_μ . We define benchmark points representing these possibilities. We then explain the new contributions from fermion/sfermion loops and their numerical behaviour. Finally we give a comparison of the new and the previously known contributions.

	BM1	BM2	BM3	BM4
μ [GeV]	350	1300	4000	-160
$\tan\beta$	40	40	40	50
M_1 [GeV]	150	150	150	140
M_2 [GeV]	300	300	300	2000
M_E [GeV]	400	400	400	200
M_L [GeV]	400	400	400	2000
$a_\mu^{1L}[10^{-10}]$	44.02	26.95	46.78	15.98

TABLE I: Definition of the benchmark points.

II. OVERVIEW OF SUSY CONTRIBUTIONS TO a_μ

Before describing the new contributions in more detail we give a brief account of the theory status of the SUSY prediction for a_μ . The one-loop contributions in Fig. 1 arise from Feynman diagrams with the exchange of the SUSY partners of the muon or neutrino, smuon $\tilde{\mu}$ or sneutrino $\tilde{\nu}_\mu$, and the SUSY partners of the neutral or charged SM bosons, the neutralinos or charginos $\tilde{\chi}^{0,\pm}$. They have been computed in the general MSSM in Ref. [33], see also [32, 34]. If all relevant SUSY masses are equal to a common scale M_{SUSY} , these contributions can be approximated by $13 \times 10^{-10} \text{sgn}(\mu) \tan\beta (100 \text{ GeV}/M_{\text{SUSY}})^2$, where μ is the Higgsino mass parameter and $\tan\beta = v_u/v_d$ is the ratio of the Higgs doublet vacuum expectation values. This clearly shows that SUSY can be the origin of the deviation (1). However, in the general case, already the one-loop contributions have an intricate parameter dependence, as shown on an analytic level in Refs. [32–35]. We illustrate this variety of possibilities at the one-loop level by Fig. 2 and define representative benchmark parameter points in Tab. I. The points are similar to the scenarios studied in Ref. [20], where it was also shown that such parameter choices, together with the squark masses defined below, are compatible with current LHC data. We use a notation similar to Ref. [32]; $M_{1,2}$ are the gaugino masses,

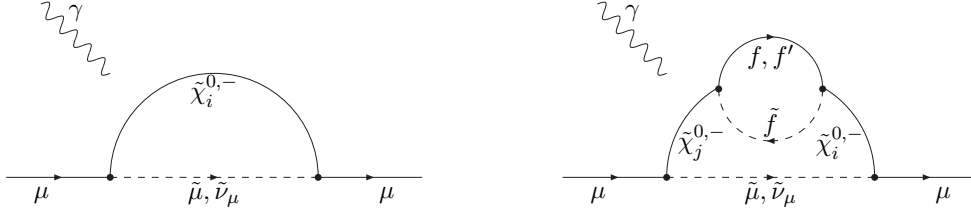


FIG. 1: SUSY one-loop diagrams and two-loop diagrams with fermion/sfermion-loop insertion. The photon can couple to each charged particle.

and the squark and slepton doublets and singlets are denoted as M_{Qi} , M_{Ui} , M_{Di} , M_{Li} , M_{Ei} , for each generation $i \in \{1, 2, 3\}$. For simplicity we choose generation-independent masses for the first two generations, $M_{E1} = M_{E2} \equiv M_E$, $M_{L1} = M_{L2} \equiv M_L$, etc., and we set all trilinear soft SUSY breaking A parameters to zero.

Fig. 2(left) shows the one-loop results a_μ^{1L} as a function of μ (the remaining parameters are chosen as in BM1–BM3). There are clearly three characteristic regions for μ , represented by the three benchmark points BM1–BM3. In the small- μ region (BM1), μ and all other masses are similar. In terms of mass-insertion diagrams (see e.g. Refs. [32, 33]), the dominant contribution is the diagram with Higgsino–wino and sneutrino exchange. The result drops with increasing μ because of the Higgsino propagator. For intermediate μ there is a minimum (BM2), and the chargino and neutralino contributions become similar. For large μ the one-loop results increase linearly in μ (BM3). In this large- μ region of parameter space all contributions involving Higgsinos are suppressed, but the mass-insertion diagram with pure bino exchange and $\tilde{\mu}_R$ - $\tilde{\mu}_L$ -transition in the smuon line is linear in μ and contributes significantly.

Fig. 2(right) shows the one-loop results as a function of M_L (where $M_2 = M_L$ and the remaining parameters are chosen as in BM4). Again, for small M_L all masses are similar and the equal-mass approximation applies. For large M_L all contributions involving $\tilde{\mu}_L$ or a sneutrino are suppressed, but the mass-insertion diagram with a purely right-handed smuon $\tilde{\mu}_R$ and

Higgsino–bino exchange is large. This contribution has the opposite sign, so μ is chosen negative to allow a positive contribution to a_μ . The benchmark point BM4 represents this large M_L -region. The possibility for such contributions with negative μ and their compatibility with dark matter constraints was also stressed recently in Ref. [36].

Our benchmark points are deliberately not optimized to give a particular value for a_μ but to represent characteristic regions of parameter space, for the following reasons. First, the result for a_μ can be adjusted easily to the value of Eq. (1) or any future measurement by tuning the values of $\tan \beta$ and the SUSY masses, without changing the characteristic of the parameter point. Second, our later two-loop results will hold in larger regions of parameter space represented by the benchmark points.

The SUSY two-loop contributions can be grouped into two classes [32]: In class 2L(a) a pure SUSY loop (of either charginos, neutralinos, or sfermions) is inserted into a SM-like diagram; these contributions have been evaluated exactly in Refs. [37, 38]. They can be large in certain regions of parameter space, but they become small as the masses of SUSY particles and/or heavy Higgs bosons become large. Diagrams of class 2L(b) involve a loop correction to a SUSY one-loop diagram. Their results are not completely known, but leading QED-logarithms [39], the full QED-corrections [40], and $(\tan \beta)^2$ -enhanced corrections [41] have been computed. Further computations of selected diagrams of classes 2L(a) and 2L(b)

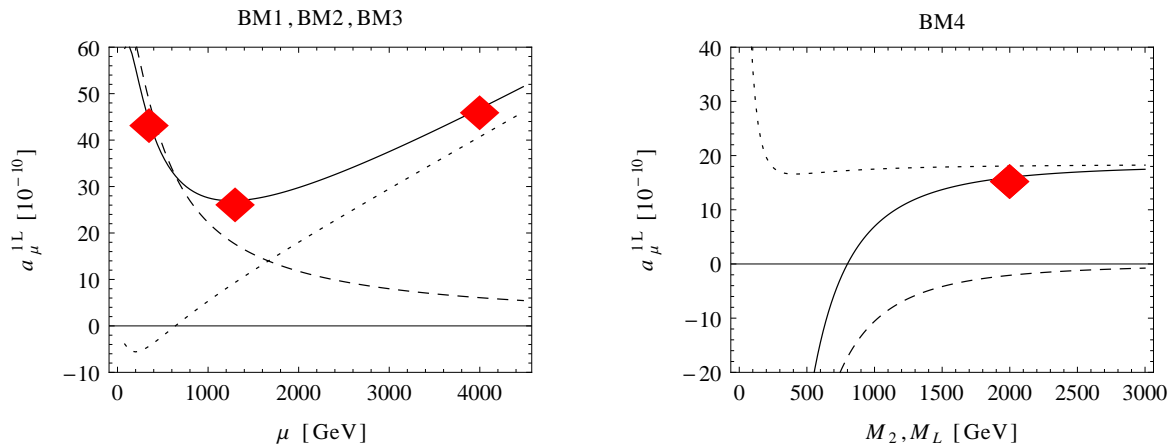


FIG. 2: Numerical results for a_μ^{1L} as a function of μ (left) and $M_2 = M_L$ (right). The other parameters are set to the values of BM1–BM3 (left) and BM4 (right). The total one-loop contribution is drawn solid, the chargino/neutralino contributions are drawn dashed/dotted, respectively. The benchmark points are indicated as red diamonds.

have been carried out in Refs. [42–45]. All known contributions of class 2L(b) can be significant corrections to the SUSY one-loop contributions.

We close the section by listing our standard values for the additional parameters that become relevant at the two-loop level, the additional squark and slepton mass parameters $M_{U,D,Q,U3,D3,Q3}$ and $M_{E3,L3}$ and the CP-odd Higgs-boson mass M_A . Where not stated otherwise, we set, like Ref. [20],

$$\begin{aligned} M_{U,D,Q,U3,D3,Q3} &= 7 \text{ TeV}, \\ M_{E3,L3} &= 3 \text{ TeV}, \\ M_A &= 1.5 \text{ TeV}. \end{aligned} \quad (2)$$

III. FERMION/SFERMION-LOOP CONTRIBUTIONS

The two-loop fermion/sfermion-loop contributions of Fig. 1 considered in the present Letter belong to the class 2L(b). Their computation represents a big step towards the full two-loop computation of a_μ in the MSSM. It is of interest to consider these contributions sep-

arately since they are gauge invariant and finite by themselves, since their evaluation is particularly challenging, and since they have a distinctive phenomenological behaviour.

The fermion/sfermion pairs in the inner loop run over all quarks and leptons of all three generations and the associated squarks and sleptons. Hence these contributions introduce a dependence of a_μ on all sfermion mass parameters for the squark and slepton doublets and singlets of all generations. With the assumption of universality of the first two generations stated above, and since the smuon mass parameters M_L and M_E appear already in the one-loop contributions, eight new free mass parameters for the inner loops come into play: $M_U, M_D, M_Q, M_{U3}, M_{D3}, M_{Q3}, M_{E3}, M_{L3}$.

Technically, the two-loop fermion/sfermion-loop diagrams involve a higher number of heavy mass scales than all previously considered two-loop contributions to a_μ in the SM and the MSSM. The SM diagrams involve up to three, the diagrams of Refs. [37, 38] up to four, the diagrams here up to five different heavy mass scales. We have computed the diagrams in

two ways — once by appropriately extending the standard techniques developed for Refs. [37, 38], and once using an iterated one-loop calculation similar to the simpler cases of Ref. [46]. A similar class of diagrams with neutralino or gluino exchange has been considered for electric dipole moments in Refs. [47, 48] in an approximation where Higgsino–gaugino mixing is neglected. In Refs. [46–48] all two-loop diagrams were ultraviolet finite, while in our case the diagrams involve subdivergences and need to be renormalized.

In addition to the genuine two-loop diagrams we consider the counterterm diagrams of Fig. 3. We use the on-shell renormalization scheme for SM and SUSY masses as in Refs. [49–53] and the $\overline{\text{DR}}$ -scheme for $\tan\beta$ [56]. The renormalization constants are computed from diagrams with either mixed fermion/sfermion-loops or pure fermion- or sfermion-loops. Adding two-loop and counterterm diagrams yields the final finite and well-defined result for the fermion/sfermion-loop contributions $a_\mu^{2\text{L},ff}$.

The full details of the calculation and analytical results will be presented in a forthcoming publication. In the following we will present and discuss the main properties of the results for $a_\mu^{2\text{L},ff}$. Their two most prominent features are:

- They contain the large and universal quantities $\Delta\alpha$ and $\Delta\rho$ from fermion and sfermion loops, see Sec. III A.
- They show non-decoupling behaviour if e.g. squark masses become large, and they contain large logarithms of ratios of squark masses over smuon, chargino and neutralino masses, see Sec. III B. This allows to find rather simple semianalytic approximations for these contributions.

A. Large universal corrections

To discuss the first point we start by noting that all SUSY one-loop contributions are

proportional to the fine-structure constant $\alpha = e^2/4\pi$ and some power of the weak mixing angle s_W or c_W . There are several motivated definitions of these quantities, e.g. α can be defined at zero momentum in the Thomson limit, or as a running $\alpha(M_Z)$ at the Z-boson mass scale, or α/s_W^2 could be eliminated in favour of the muon decay constant G_F . Here, $\alpha(M_Z) = \alpha/(1 - \Delta\alpha(M_Z))$, and the shift $\Delta\alpha(M_Z)$ is defined via fermion-loop contributions to the photon vacuum polarization, see Ref. [4] for a recent evaluation. Using G_F effectively amounts to using $\alpha(G_F) = \alpha(1 + \Delta r)$, where Δr summarizes quantum corrections to muon decay. The leading contributions to Δr are given by $\Delta\alpha(M_Z)$ and the fermion- and sfermion-loop contributions to the quantity $\Delta\rho$, see Ref. [57] for definitions and a precise MSSM evaluation. Inserted into $a_\mu^{1\text{L}}$, the differences are numerically sizeable, and this ambiguity is an inherent source of theory uncertainty of the one-loop calculation. However, the differences are formally of two-loop order, and in a full two-loop calculation the differences will be compensated by corresponding differences in the definitions of the renormalization constant δe .

The point is that the differences arise mainly from $\Delta\alpha(M_Z)$ and $\Delta\rho$ — and thus from fermion and sfermion loops. So it is precisely our new class of two-loop contributions to a_μ which eliminates the one-loop parametrization ambiguity. The full two-loop result is insensitive to the choice of parametrization, up to subleading contributions to Δr and three-loop effects. In our calculation we choose to parametrize the one-loop result in terms of $\alpha(M_Z)$, which leads to the simplest structure of the renormalization constants and the smallest values of the two-loop contributions.

Tab. II shows the numerical impact of the one-loop parametrization ambiguity compared to our full two-loop result, for the cases of the benchmark points. The first rows show the three different one-loop results obtained from the three indicated definitions of α ; the last

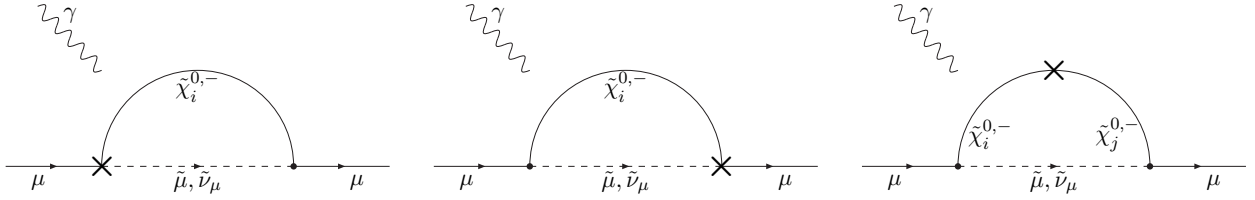


FIG. 3: Relevant counterterm diagrams with counterterm insertions at the external muon vertex or in the chargino/neutralino self energy. The photon can couple to each charged particle.

	BM1	BM2	BM3	BM4
$a_\mu^{1L}(\alpha)$	41.42	25.36	44.02	15.03
$a_\mu^{1L}(\alpha(G_F))$	42.92	26.28	45.62	15.58
$a_\mu^{1L}(\alpha(M_Z))$	44.02	26.95	46.78	15.98
$a_\mu^{1L} + a_\mu^{2L,ff}$	45.82	28.16	48.98	16.76

TABLE II: One-loop results for different choices of the fine-structure constant α and our two-loop results, which remove the one-loop ambiguity. The results are given in units of 10^{-10} .

row shows the sum of the one-loop result and our new two-loop contributions, consistently parametrized in terms of $\alpha(M_Z)$. The size of the intervals spanned by the different one-loop results is 6%. The two-loop contributions are between 4% and 5% of the respective one-loop contributions. It is not surprising that the two-loop contributions are similarly large as the size of these one-loop intervals; but it is noteworthy that in all cases the full two-loop result is significantly *outside* the one-loop intervals. This highlights the importance of the fermion/sfermion-loop contributions, beyond merely reducing the theory uncertainty.

B. Parameter dependence and non-decoupling behaviour

Next we focus on the parameter dependence of the new two-loop contributions. As discussed above, in our analysis there are eight free mass parameters for the inner loops, in addition to the parameters already present at the one-loop level.

Motivated by the LHC results discussed in the introduction, we allow split spectra and vary all the eight mass parameters separately over the wide range from 1...1000 TeV. Fig. 4 shows the resulting two-loop corrections for the case of benchmark point BM1, where one mass parameter is varied at a time and the others are fixed at their standard values. The non-decoupling, logarithmic dependence on all the sfermion masses is apparent. For this benchmark point and the chosen sfermion mass range, the two-loop corrections can have both signs and can be as large as 10% or -5% of the one-loop contributions.

More generally, the results for sufficiently heavy sfermions can be well approximated by leading logarithms. We obtain the semianalytical expression

$$\frac{a_\mu^{2L,ff}}{a_\mu^{1L}} \approx b_0 + \sum_{\tilde{q}} b_{\tilde{q}} \log \frac{M_{\tilde{q}}}{7 \text{ TeV}} + \sum_{\tilde{l}} b_{\tilde{l}} \log \frac{M_{\tilde{l}}}{3 \text{ TeV}}, \quad (3)$$

where the sums extend over the squarks $\tilde{q} = Q, U, D, Q3, U3, D3$ and the sleptons $\tilde{l} = L3, E3$, respectively. The coefficients $b_0, b_{\tilde{q}}, b_{\tilde{l}}$ implicitly depend on the one-loop parameters in a complicated way, but the dependence on the eight two-loop parameters is made explicit. We have verified that this approximation is valid for all benchmark points provided the sfermion masses are above around 5 TeV. Instead of repeating Fig. 4 for all benchmark points we provide Tab. III with all necessary coefficients.

The physical reason for the non-decoupling

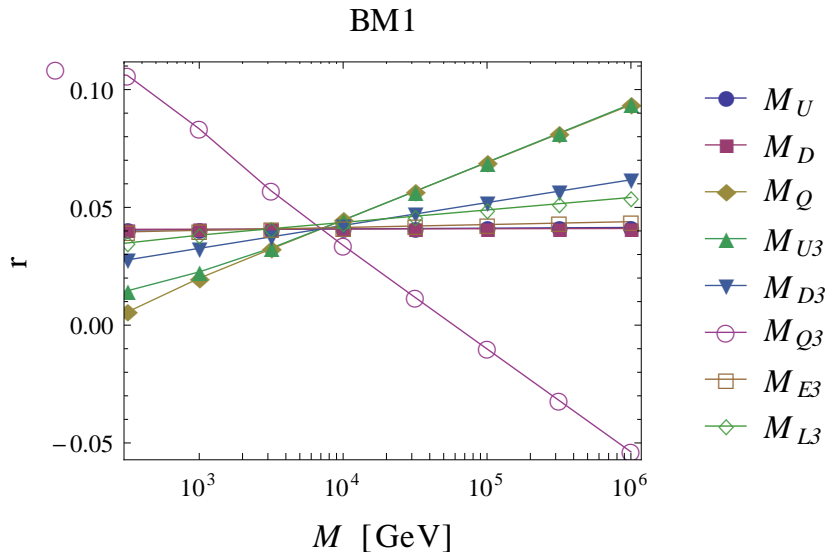


FIG. 4: Relative correction $r \equiv a_{\mu}^{2L, f\bar{f}}/a_{\mu}^{1L}$ from fermion/sfermion loops for benchmark point BM1 as a function of each sfermion mass parameter.

behaviour is that the effective theory obtained by integrating out a heavy sfermion is not supersymmetric any more. Gaugino and Higgsino interactions can differ from the corresponding gauge and Yukawa interactions by matching constants which contain large logarithms of the heavy sfermion mass. For gaugino interactions these non-decoupling matching corrections are known as superoblique corrections, and Refs. [58–60] have given analytical results for the coefficients of the large logarithms for several cases. The results are proportional to the square of the gauge couplings of the heavy sfermion. Likewise, the matching corrections to the Higgsino interactions (analytical results for heavy squarks can be found in Ref. [61]) contain large logarithms times the square of the sfermion Yukawa coupling. This knowledge allows a qualitative understanding of the results of Fig. 4 and Tab. III.

The top and bottom Yukawa couplings are the largest couplings of the inner loop, followed by the tau Yukawa and the SU(2) and U(1) gauge couplings. The first/second generation

Yukawa couplings are negligible. In BM1, the Higgsino–wino contribution dominates at the one-loop level. Hence, the slopes of the M_{Q3} , M_{U3} lines in Fig. 4 are largest because of the large top Yukawa coupling to the Higgsino. The slope of the M_Q line is also large since the left-handed squarks couple to the wino. The slopes of the M_U , M_D lines are particularly small since the 1st/2nd generation singlets have neither significant Yukawa couplings nor SU(2) gauge interactions.

As the parameters are changed from BM1 to BM2 and BM3, the Higgsino–wino contribution becomes less, the pure bino contribution more important. Clearly, the non-decoupling logarithms to the bino contributions are controlled by the small U(1) gauge couplings and the hypercharges. We have verified that for a parameter point where the bino contribution dominates sufficiently strongly, the coefficients of the logarithms indeed become generation-independent and proportional to the squared hypercharge of the respective sfermion. For our point BM3, only the coefficients b_U , b_D , b_{E3} have this be-

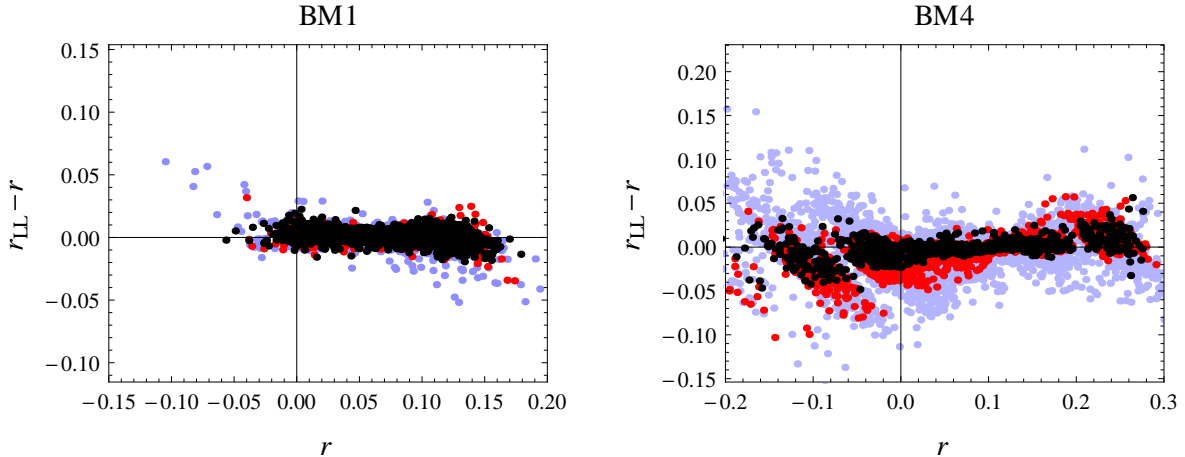


FIG. 5: The exact result for $r \equiv a_\mu^{2L, f\bar{f}}/a_\mu^{1L}$ compared with the approximation r_{LL} given by the r.h.s. of Eq. (3) together with the coefficients in Tab. III. The mass parameters are chosen randomly around the benchmark points BM1 and BM4, with the ranges given in the text.

	BM1	BM2	BM3	BM4
b_0	0.0408	0.0446	0.0469	0.0490
b_Q	0.0106	0.0060	0.0014	-0.0011
b_U	0.0001	0.0013	0.0025	0.0031
b_D	0.0000	0.0003	0.0006	0.0008
b_{Q3}	-0.0190	-0.0106	-0.0019	0.0355
b_{U3}	0.0107	0.0069	0.0025	-0.0448
b_{D3}	0.0042	0.0024	0.0007	0.0075
b_{L3}	0.0023	0.0015	0.0007	0.0014
b_{E3}	0.0005	0.0008	0.0010	0.0018

TABLE III: Coefficients of Eq. (3) for benchmark points BM1–BM4.

haviour. The other coefficients also receive non-negligible corrections from the Higgsino–wino contributions, which are about 7 times smaller than the bino contribution but involve much larger corrections similar to the case of BM1. Nevertheless, this explains the overall decrease of the slopes for BM2 and BM3.

The case of BM4 is similar to the one of BM1, except that at the one-loop level the Higgsino–bino contribution dominates, instead of the Higgsino–wino contribution. The relative

corrections from top-Yukawa enhanced contributions are larger for BM4, and therefore the slopes for $\log M_{Q3, U3}$ are even larger for BM4 than for BM1.

The validity of the approximation (3) and the coefficients in Tab. III goes far beyond the pure benchmark points, because the benchmark points are representative for larger regions of parameter space with characteristic properties. Whenever we choose a parameter point similar to one of the benchmark points, we can still use Eq. (3) with the coefficients given in the table. The quality of the approximation is quantified in Fig. 5. It shows the difference of the exact result and the approximation by Eq. (3) for randomly chosen parameter points scattered around the benchmark points. The parameter ranges for the light blue points are given in Tab. IV. We also impose the constraints $a_\mu^{1L} \geq 5 \times 10^{-10}$ and $|M_2 - \mu| \geq 5$ GeV to avoid artificially large effects due to accidental cancellations. The other eight sfermion-mass parameters are varied in the range $[10^3, 10^6]$ GeV. For the red and black points the further constraints given in Tab. V are successively applied. These further constraints strengthen the equal-mass characteristic of the BM1 region and the decoupling of the wino and

	BM1	BM4
μ [GeV]	[100,200]	[-200,-100]
M_1 [GeV]	[100,200]	[100,200]
M_2 [GeV]	[200,400]	[1000,3000]
M_E [GeV]	[200,500]	[100,300]
M_L [GeV]	[200,500]	[1000,3000]

TABLE IV: Scan intervals for the least restrictive light blue parameter regions.

	BM1	BM4
red	$M_{E,L} \leq 400$	$M_2, M_L \geq 2000,$ $M_1 \leq \mu + 40$
black	$M_{E,L} \geq 250$	$M_1 \leq \mu - 10$

TABLE V: Additional parameter constraints for the red and black parameter regions (in GeV).

$\tilde{\mu}_L$ in the BM4 region.

In the most restrictive black region, the parameters can fluctuate within a factor ~ 1.5 around the benchmark points. In this region, the approximation is generally good. For the red and light blue parameter regions, the approximation becomes gradually worse, but even in the largest region, the approximation works well for the majority of parameter points. We only show the results for BM1 and BM4; for the other benchmark points the corrections are smaller and the approximation works even better.

The figure also shows the generally possible magnitude of the fermion/sfermion-loop corrections. Already within the most restrictive considered parameter regions, the corrections are up to 15% and 30% of the respective one-loop result for BM1, BM4, respectively.

C. Comparison with other MSSM two-loop contributions

Finally we summarize the behaviour of the fermion/sfermion-loop contributions and compare it with all previously known two-loop contributions to a_μ in the MSSM. Fig. 6 shows the results for the benchmark points as functions of various motivated combinations of sfermion masses: either of a common third generation sfermion mass $M_{U3,D3,Q3,E3,L3} \equiv M$, or of a universal squark mass $M_{U,D,Q} \equiv M$, or, as an example with particularly large corrections, purely as a function of M_{Q3} with M_{U3} fixed to 1 TeV. Each time, the non-varied sfermion masses are kept at their standard values.

As is well known, the photonic contributions [40] and the $(\tan \beta)^2$ -enhanced contributions [41] are both large. The photonic contributions are around -8% for the benchmark points BM1–BM3 and around -7% for BM4 due to its smaller mass scales. The $(\tan \beta)^2$ -enhanced contributions have a non-trivial parameter dependence, in particular their sign changes when going from BM1 to either BM3 or BM4. Their magnitude is up to 7% in our examples. Because of the heavy Higgs-boson mass the contributions of class 2L(a) are small. Even though they have a dependence on the sfermion masses, due to decoupling in these contributions the dependence is invisible in the plots.

The new fermion/sfermion-loop contributions are always in the few-percent range and can even become the largest two-loop contributions. For the cases of universal squark mass and of common third-generation sfermion masses we find between 5% and 10% corrections. For the considered case with larger mass splittings, $M_{Q3} \gg M_{U3}$, the corrections are even more significant, and their parameter dependence is very strong. There can be negative corrections for BM1 and BM2. For BM4, the corrections are positive and around 15% for squark masses up to 20 TeV; outside the plot, the corrections grow beyond 30% for squark masses

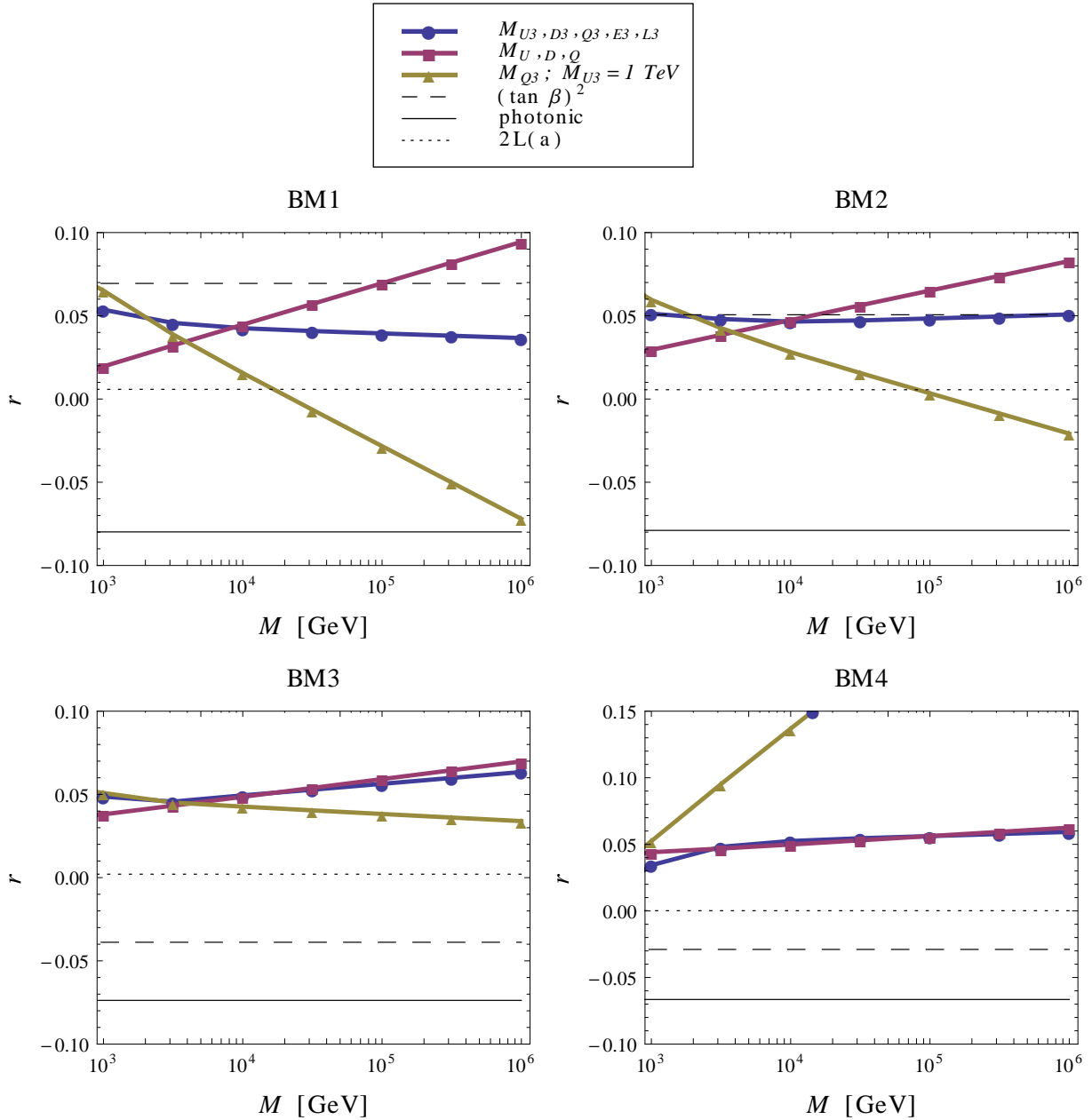


FIG. 6: Results for the ratios $r \equiv a_\mu^{2L}/a_\mu^{1L}$ for the known MSSM two-loop contributions to a_μ , for all benchmark points. The thick, coloured lines show the new fermion/sfermion-loop contributions for the combinations of sfermion masses indicated in the legend. The thin lines show the previously known $(\tan \beta)^2$ (dashed), photonic (solid), and $2L(a)$ (dotted) contributions. The sfermion mass dependence of the $2L(a)$ contributions is negligible and invisible in the plots.

up to 1000 TeV.

IV. CONCLUSIONS

Large contributions to a_μ are possible in a variety of qualitatively different parameter regions of the MSSM. To illustrate this we defined benchmark parameter points which represent these regions with large a_μ and which are compatible with limits from the LHC.

We then presented results of a new calculation of fermion/sfermion-loop contributions to a_μ in the MSSM. These will be important for a correct interpretation of current or future a_μ measurements within the MSSM and for drawing precise conclusions on preferred parameter regions. The new corrections introduce a dependence of a_μ on all sfermion masses beyond the smuon masses, and they can be surprisingly large. For moderate sfermion masses they are typically around 4%–5% but can also reach up to 10%, as Fig. 4 exemplifies. If the additional sfermion masses are in the multi-TeV range, the corrections grow logarithmically similar to the so-called superoblique corrections; in our examples up to 30% corrections are possible particularly in scenarios with large splitting between left- and right-handed stop masses.

Semianalytical expressions are provided which can be easily evaluated in practical applications to obtain good estimates of the new contributions. Together with the formulas provided in Refs. [40, 41], this allows a compact implementation of a good approximation of the MSSM two-loop contributions to a_μ .

Taking into account the fermion/sfermion-loop contributions removes the ambiguity from parametrizing the one-loop contributions either in terms of α , $\alpha(M_Z)$, or G_F . The full result including the two-loop corrections is typically outside the interval spanned by the differently parametrized one-loop results, highlighting the importance of the new corrections.

Finally, we have illustrated the non-trivial parameter dependence of the new fermion/sfermion-loop corrections and the previously known two-loop contributions. Both the fermion/sfermion-loop and the $(\tan\beta)^2$ corrections can be positive or negative, and either of them can be larger in magnitude than the photonic contributions. Each of these new and previously known two-loop corrections can be larger than the future experimental uncertainty.

The present Letter focuses on the most prominent features of the fermion/sfermion-loop corrections. A discussion of the deviations from the leading logarithmic behaviour and the influence of squark mixing, together with the full details of the calculation and analytical results, will be presented in a forthcoming publication.

Acknowledgements

We acknowledge financial support by the German Research Foundation DFG through Grant No. STO876/1-1, by DAAD and by CNPq. HF thanks TU Dresden and IKTP for their hospitality.

-
- [1] G.W. Bennett, et al., (Muon $(g - 2)$ Collaboration), Phys. Rev. D **73**, 072003 (2006).
 - [2] C. Gnendiger, D. Stöckinger and H. Stöckinger-Kim, Phys. Rev. D **88** (2013) 053005 [arXiv:1306.5546 [hep-ph]].
 - [3] M. Davier, A. Hoecker, B. Malaescu and Z. Zhang, Eur. Phys. J. C **71** (2011) 1515 [Erratum-ibid. C **72** (2012) 1874] [arXiv:1010.4180 [hep-ph]].
 - [4] K. Hagiwara, R. Liao, A. D. Martin, D. Nomura and T. Teubner, J. Phys. G G **38** (2011) 085003 [arXiv:1105.3149 [hep-ph]].
 - [5] M. Benayoun, P. David, L. DelBuono and F. Jegerlehner, Eur. Phys. J. C **73** (2013) 2453

- [arXiv:1210.7184 [hep-ph]].
- [6] J. Miller, E. de Rafael, B.L. Roberts, D. Stöckinger, *Ann.Rev.Nucl.Part.Sci* **62** (2012) 237.
- [7] R. Benbrik, M. Gomez Bock, S. Heinemeyer, O. Stal, G. Weiglein and L. Zeune, *Eur. Phys. J. C* **72**, 2171 (2012) [arXiv:1207.1096 [hep-ph]].
- [8] A. Arbey, M. Battaglia, A. Djouadi and F. Mahmoudi, *JHEP* **1209**, 107 (2012) [arXiv:1207.1348 [hep-ph]].
- [9] P. Bechtle, T. Bringmann, K. Desch, H. Dreiner, M. Hamer, C. Hensel, M. Kramer and N. Nguyen *et al.*, *JHEP* **1206** (2012) 098 [arXiv:1204.4199 [hep-ph]].
- [10] C. Balazs, A. Buckley, D. Carter, B. Farmer and M. White, arXiv:1205.1568 [hep-ph].
- [11] O. Buchmueller, R. Cavanaugh, M. Citron, A. De Roeck, M. J. Dolan, J. R. Ellis, H. Flacher and S. Heinemeyer *et al.*, *Eur. Phys. J. C* **72** (2012) 2243 [arXiv:1207.7315 [hep-ph]].
- [12] H. Baer, V. Barger, P. Huang and X. Tata, *JHEP* **1205** (2012) 109 [arXiv:1203.5539 [hep-ph]].
- [13] M. Papucci, J. T. Ruderman and A. Weiler, *JHEP* **1209** (2012) 035 [arXiv:1110.6926 [hep-ph]].
- [14] T. J. LeCompte and S. P. Martin, *Phys. Rev. D* **85** (2012) 035023 [arXiv:1111.6897 [hep-ph]].
- [15] H. Murayama, Y. Nomura, S. Shirai and K. Tobioka, *Phys. Rev. D* **86** (2012) 115014 [arXiv:1206.4993 [hep-ph]].
- [16] M. Endo, K. Hamaguchi, K. Ishikawa, S. Iwamoto and N. Yokozaki, *JHEP* **1301** (2013) 181 [arXiv:1212.3935 [hep-ph]].
- [17] M. Endo, K. Hamaguchi, S. Iwamoto and N. Yokozaki, *Phys. Rev. D* **84** (2011) 075017 [arXiv:1108.3071 [hep-ph]].
- [18] T. Moroi, R. Sato and T. T. Yanagida, *Phys. Lett. B* **709** (2012) 218 [arXiv:1112.3142 [hep-ph]].
- [19] M. Endo, K. Hamaguchi, S. Iwamoto, K. Nakayama and N. Yokozaki, *Phys. Rev. D* **85** (2012) 095006 [arXiv:1112.6412 [hep-ph]].
- [20] M. Endo, K. Hamaguchi, S. Iwamoto and T. Yoshinaga, arXiv:1303.4256 [hep-ph].
- [21] M. Ibe, S. Matsumoto, T. T. Yanagida and N. Yokozaki, *JHEP* **1303** (2013) 078 [arXiv:1210.3122 [hep-ph]].
- [22] G. Bhattacharyya, B. Bhattacharjee, T. T. Yanagida and N. Yokozaki, arXiv:1304.2508 [hep-ph].
- [23] T. Cheng and T. Li, *Phys. Rev. D* **88** (2013) 015031 [arXiv:1305.3214 [hep-ph]].
- [24] M. Ibe, T. T. Yanagida and N. Yokozaki, *JHEP* **1308** (2013) 067 [arXiv:1303.6995 [hep-ph]].
- [25] S. Mohanty, S. Rao and D. P. Roy, arXiv:1303.5830 [hep-ph].
- [26] S. Akula and P. Nath, *Phys. Rev. D* **87**, **115022** (2013) [arXiv:1304.5526 [hep-ph]].
- [27] J. L. Evans, M. Ibe, S. Shirai and T. T. Yanagida, *Phys. Rev. D* **85** (2012) 095004 [arXiv:1201.2611 [hep-ph]].
- [28] R. M. Carey, K. R. Lynch, J. P. Miller, B. L. Roberts, W. M. Morse, Y. K. Semertzides, V. P. Druzhinin and B. I. Khazin *et al.*, FERMILAB-PROPOSAL-0989.
- [29] B. L. Roberts, *Chin. Phys. C* **34** (2010) 741 [arXiv:1001.2898 [hep-ex]].
- [30] H. Iinuma [J-PARC New g-2/EDM experiment Collaboration], *J. Phys. Conf. Ser.* **295** (2011) 012032.
- [31] D. W. Hertzog, J. P. Miller, E. de Rafael, B. Lee Roberts and D. Stöckinger, arXiv:0705.4617.
- [32] D. Stöckinger, *J. Phys. G* **34** (2007) R45.
- [33] T. Moroi, *Phys. Rev. D* **53** (1996) 6565 [Erratum-ibid. **56** (1997) 4424].
- [34] S. Martin and J. Wells, *Phys. Rev. D* **64** (2001) 035003.
- [35] G. -C. Cho, K. Hagiwara, Y. Matsumoto and D. Nomura, *JHEP* **1111** (2011) 068 [arXiv:1104.1769 [hep-ph]].
- [36] P. Grothaus, M. Lindner and Y. Takanishi, *JHEP* **1307** (2013) 094.
- [37] S. Heinemeyer, D. Stöckinger and G. Weiglein, *Nucl. Phys. B* **690** (2004) 62.
- [38] S. Heinemeyer, D. Stöckinger and G. Weiglein, *Nucl. Phys. B* **699** (2004) 103.

- [39] G. Degrassi and G. F. Giudice, *Phys. Rev. D* **58** (1998) 053007.
- [40] P. von Weitershausen, M. Schafer, H. Stockinger-Kim and D. Stockinger, *Phys. Rev. D* **81** (2010) 093004 [arXiv:1003.5820 [hep-ph]].
- [41] S. Marchetti, S. Mertens, U. Nierste and D. Stöckinger, *Phys. Rev. D* **79**, 013010 (2009) [arXiv:0808.1530 [hep-ph]].
- [42] T. F. Feng, L. Sun and X. Y. Yang, *Phys. Rev. D* **77** (2008) 116008 [arXiv:0805.0653 [hep-ph]].
- [43] T. F. Feng, L. Sun and X. Y. Yang, *Nucl. Phys. B* **800** (2008) 221 [arXiv:0805.1122 [hep-ph]].
- [44] T. F. Feng and X. Y. Yang, *Nucl. Phys. B* **814** (2009) 101 [arXiv:0901.1686 [hep-ph]].
- [45] T. F. Feng, X. Q. Li, L. Lin, J. Maalampi and H. S. Song, *Phys. Rev. D* **73**, 116001 (2006).
- [46] S. M. Barr and A. Zee, *Phys. Rev. Lett.* **65** (1990) 21 [Erratum-ibid. **65** (1990) 2920].
- [47] N. Yamanaka, arXiv:1212.5800 [hep-ph].
- [48] N. Yamanaka, *Phys. Rev. D* **87** (2013) 011701 [arXiv:1211.1808 [hep-ph]].
- [49] A. Denner, *Fortschr. d. Physik*, **41** (1993) 4
- [50] W. Hollik, E. Kraus, M. Roth, C. Rupp, K. Sibold and D. Stöckinger, *Nucl. Phys. B* **639** (2002) 3.
- [51] T. Fritzsche and W. Hollik, *Eur. Phys. J. C* **24**, 619 (2002).
- [52] W. Hollik and H. Rzehak, *Eur. Phys. J. C* **32** (2003) 127.
- [53] We thank T. Hahn and the authors of Refs. [54, 55] for providing us with a preliminary model file implementing this renormalization scheme.
- [54] S. Heinemeyer, H. Rzehak and C. Schappacher, *Phys. Rev. D* **82** (2010) 075010 [arXiv:1007.0689 [hep-ph]].
- [55] T. Fritzsche, S. Heinemeyer, H. Rzehak and C. Schappacher, *Phys. Rev. D* **86** (2012) 035014 [arXiv:1111.7289 [hep-ph]].
- [56] A. Freitas and D. Stockinger, *Phys. Rev. D* **66** (2002) 095014 [hep-ph/0205281].
- [57] S. Heinemeyer, W. Hollik, D. Stockinger, A. M. Weber and G. Weiglein, *JHEP* **0608** (2006) 052 [hep-ph/0604147].
- [58] H. -C. Cheng, J. L. Feng and N. Polonsky, *Phys. Rev. D* **56** (1997) 6875 [hep-ph/9706438].
- [59] E. Katz, L. Randall and S. -f. Su, *Nucl. Phys. B* **536** (1998) 3 [hep-ph/9801416].
- [60] S. Kiyoura, M. M. Nojiri, D. M. Pierce and Y. Yamada, *Phys. Rev. D* **58** (1998) 075002 [hep-ph/9803210].
- [61] P. H. Chankowski, *Phys. Rev. D* **41** (1990) 2877.